Comparative Analysis of Mitogenomes of *Microtendipes* (Diptera: Chironomidae) and Its Phylogenetic Implications

Chao Song , Yiyi Wang , Wenji Wang , Teng Lei , Xin Qi * , Luxian Li *

Posted Date: 26 April 2025

doi: 10.20944/preprints202504.2155.v1

Keywords: Mitogenome; Chironomidae; Phylogeny; *Microtendipes*

 doi:10.20944/preprints202504.2155.v1

Article

Comparative Analysis of Mitogenomes of *Microtendipes* (Diptera: Chironomidae) and Its Phylogenetic Implications

Chao Song [1], Yiyi Wang [1], Wenji Wang [1], Teng Lei [1], Xin Qi [1,*] and Luxian Li [2,*]

[1] Zhejiang Provincial Key Laboratory of Plant Evolutionary Ecology and Conservation, School of Life Sciences, Taizhou University, Taizhou 318000, China; songchaonk@163.com (C.S.); leiteng@tzc.edu.cn (T.L.)

[2] Zhejiang Environment Technology Co., Ltd, Taizhou 318000, China

* Correspondence: qixin0612@tzc.edu.cn (X.Q.); luxianli221@163.com (L.L.)

Abstract: Insect mitochondrial genomes are pivotal for understanding evolutionary relationships and species identification. This study focuses on *Microtendipes* (Chironomidae), a genus with unresolved phylogenetic positioning and cryptic species challenges. We sequenced and analyzed eight mitogenomes from five *Microtendipes* species, integrating 18 published Chironominae mitogenomes to reconstruct phylogenies using Maximum Likelihood and Bayesian Inference. The mitogenomes exhibited conserved gene arrangements but variable control region lengths (338–1,266 bp) and high AT content (94.14–96.42% in control regions). Comparative analyses revealed significant intraspecific genetic distances (5.3–13.8% across 13 protein-coding genes), challenging COI-based barcoding for species delimitation. Phylogenetic reconstructions resolved *Microtendipes* as a distinct clade, refuting its inclusion in the *Polypedilum* complex. Notably, larval morphology-based species groupings conflicted with molecular data, suggesting cryptic diversity. Our results support *Microtendipes* as a potential independent tribe within Chironominae, highlighting mitogenomes' utility in resolving taxonomic uncertainties. This study advances the evolutionary understanding of Chironomidae and underscores the limitations of single-gene barcodes in species-rich genera.

Keywords: Mitogenome; Chironomidae; Phylogeny; *Microtendipes*

1. Introduction

Insect mitochondrial genomes are typically circular molecules ranging in size from 14 to 20 kilobases (kb), encoding a conserved arrangement of 13 protein-coding genes (PCGs), 22 transfer RNAs (tRNAs), and two ribosomal RNAs (rRNAs) in a characteristic order and orientation across most insect orders [1]. These genomes have proven instrumental in diverse fields, including species identification [2-4] and population genetics [5-6]. This is due to their advantages, which stem from maternal inheritance, rapid substitution rates, and ease of accessibility [7]. Moreover, investigating mitochondrial genome characteristics, such as nucleotide composition, codon usage, evolutionary rates, and secondary structures of RNA genes, has significantly contributed to a deeper understanding of the evolutionary trajectories of diverse organismal groups [8-13]. Within the insect family Chironomidae, mitogenomes have been extensively utilized in studies aimed at elucidating phylogenetic relationships within the family and exploring its evolutionary history [14-17].

Chironomidae, normally known as non-biting midges, exhibit the greatest diversity of species that have evolved to thrive under extreme abiotic environments. These include species capable of enduring a wide range of temperatures, from extremely low temperatures to extremely high temperatures, as well as those resilient to oxygen scarcity, high levels of salinity, both acidic and alkaline conditions (low and high pH), and even complete desiccation [18-19]. Their remarkable adaptability allows them to inhabit an extensive range of habitats, spanning from the frigid, glacier-

 doi:10.20944/preprints202504.2155.v1

covered peaks of the tallest mountains to the depths of freshwater bodies, demonstrating their remarkable versatility and resilience in diverse environments [20-21].

Microtendipes Kieffer, 1915, a genus of the tribe Chironomini in the subfamily Chironominae, exhibits a cosmopolitan distribution across all zoogeographical regions [22]. Its immature stages are predominantly found within littoral and sublittoral sediments of vast aquatic habitats, with a limited number of species also inhabiting flowing water environments. The extensive variability in body colors, encompassing thoracic, leg, and wing pigmentation, poses challenges in defining species solely based on color pattern changes [23]. DNA barcode data are pivotal in supporting the interpretation of pigmentation variations as interspecific differences [24].

Previous studies have employed morphological analysis and molecular markers to investigate species delimitation and phylogeny within *Microtendipes* [22-24], yet certain questions remain unaddressed. Firstly, a complex scenario arises when samples displaying identical color patterns form distinct clades on the evolutionary tree based on COI (cytochrome oxidase subunit I) gene sequences, accompanied by significant genetic distances, rendering species delimitation uncertain. There is debate regarding the appropriateness of classifying deeply divergent specimens, forming paraphyletic groups in COI-based phylogenetic trees, as the same species, as suggested by Song et al. (2024) [24]. This underscores the need for unexplored avenues such as the application of mitogenomes to elucidate phylogenetic relationships. Prior to this investigation, only a single *Microtendipes* species had been documented with a mitogenome [25], and no comparative analysis of nucleotide composition or evolutionary rates within the genus had been conducted. Secondly, the phylogenetic position of *Microtendipes* has long been a subject of controversy. Sæther (1977) constructed a phylogenetic tree based on female chironomid characteristics, placing this genus within Chironomini [26]. In the phylogenetic tree, *Microtendipes* formed a monophyletic group with *Paratendipes* Kieffer /*Nilothauma* Kieffer, leading to the suggestion of establishing these genera as a fourth subfamily-level taxonomic unit. However, when Sasa (1989) documented the chironomid fauna of Japan, he placed *Microtendipes* within the *Polypedilum* complex (including *Nilothuma* and *Paratendipes*), belonging to the Chironomini [27]. When molecular data were introduced, Cranston et al. (2012) supported the grouping of *Microtendipes* with several related genera (excluding *Paratendipes*) into a generic group, which formed a sister relationship with Pseudochironomini [28].

In this study, we have presented eight specimens belonging to five species of *Microtendipes*, specifically *M. bimaculatus*, *M. baishanzuensis*, *M. wuyiensis*, *M. robustus*, and *M. tuberosus*. Following this, we conducted a thorough analysis of their mitogenomic characteristics. By incorporating previously documented mitogenomes into our analysis, we reconstructed the phylogenetic evolution of the Chironominae using a comprehensive dataset comprising 25 mitochondrial genomes. To achieve this, we employed both Maximum Likelihood (ML) and Bayesian Inference (BI) methodologies, enabling us to accurately determine the phylogenetic positioning of *Microtendipes* within the subfamily.

2. Materials and Methods

2.1. Taxon Sampling and Sequencing

All the samples of *Microtendipes* individuals were collected from Baishanzu National Reserve and Wuyi Mountain National Reserve in the year of 2021 and 2022 except *Microtendipes bimaculatus*-Clade1 (MZ981734) retrieved from our previous study [25]. Targeted specimens were dissected and mounted into Euparal except the tissues for total genomic DNA extraction (thorax, head and a pair of legs). The extraction procedure followed the Qiagen DNeasy Blood and Tissue kit except for elusion buffer ranging from 100-150 μl according to different body size. The exoskeletons of thorax were cleared and mounted on corresponding voucher. A segment of cox1-5P for each species was amplified with primer pair LCO1490-L and HCO2198-L [29] and sequenced with Sanger sequencing as described by Song et al. (2018) [30], and further confirmed the identification. The genomic DNA was subsequently pooled and sequenced using the Illumina Novaseq 6000 (PE150, Ullumina, San Diego, CA) platform.

 doi:10.20944/preprints202504.2155.v1

Multi softwares, Mitoz (v3.4) [31], NOVOPlasty (v4.3.1) [32] and SPAdes (v4.0.0) [33], were employed to assemble the reads, and the results of three assemblers were used to revise each other to obtain accurate mito genomes. The mito genomes were annotated using MITOS2 (v2.1.7) [34] and then visualized using java package CGView (v2.0.3) [35].

2.2. Genome Composition and Codon Usage

The base composition was analyzed utilizing seqkit (v2.3.0) [36]. The codon usage of PCGs were analyzed using EMBOSS (v6.6.0.0) [37] and python module codonw-slim (v1.5.0). The figures about codons of PCGs were generated using R package ggplot2 (v3.5.1) [38].

2.3. Substitution Rate and Phylogenetic Analyses

The mitochondrial genomes of species listed in Table 1, including the eight newly sequenced mitogenomes reported in this study, were selected for phylogenetic reconstruction. *Rheocricotopus villiculus* (MW373526) was designated as the outgroup. The thirteen protein-coding genes (PCGs) were aligned using MAFFT (version 7.505) [39], with all stop codons retained and indels removed during the process. Subsequent to alignment, all sequences were manually reviewed, corrected, and concatenated for further analyses. Pairwise genetic distances among the 13 PCGs were computed using MEGA11 [40]. Statistical comparisons of genetic distances were conducted using the Friedman test in R, with multiple pairwise comparisons performed using the Wilcoxon rank-sum test, and p-values adjusted using the Benjamini-Hochberg (BH) method to control for false discovery rate. The resulting boxplot was generated using the R package ggplot2.

Table 1. List of the mitochondrial genomes analyzed in the present study, * means from this study.

Species	Accession No.	Species	Accession No.
Axarus fungorum	ON099430	*Demicryptochironomus minus*	PQ014456
Chironomus kiiensis	MZ150770	*Cryptochironomus defectus*	PQ014461
Microchironomus tabarui	MZ261913	*Cladopelma edwardsi*	PQ014460
Microtendipes bimaculatus-Clade1	MZ981734	*Dicrotendipes* sp.	ON838257
Microtendipes bimaculatus-Clade2	PP966948*	*Einfeldia* sp.	ON943041
Microtendipes bimaculatus-Clade3	PP966952*	*Endochironomus pekanus*	OP950228
Microtendipes bimaculatus-Clade3	PP966953*	*Glyptotendipes tokunagai*	MZ747091
Microtendipes baishanzuensis	PP966947*	*Microchironomus tener*	ON975027
Microtendipes tuberosus	PP966949*	*Phaenopsectra flavipes*	OP950216
Microtendipes wuyiensis	PP966951*	*Sergentia baueri*	OP950220
Microtendipes robustus	PP966950*	*Stictochironomus akizukii*	OP950218
Microtendipes robustus	PP966954*	*Synendotendipes impar*	OP950223
Polypedilum henicurum	MZ981735	*Synendotendipes* sp.1	OP950221

A total of four datasets were concatenated for phylogenetic analyses, namely: (i) a PCG matrix comprising all thirteen protein-coding genes (PCGs) totaling 11,094 base pairs (bp), (ii) a PCGrRNA matrix incorporating the thirteen PCGs and the two ribosomal RNA (rRNA) genes, amounting to 12,643 bp, (iii) a PCG12 matrix containing the first and second codon positions of the thirteen PCGs, and (iv) a PCG12rRNA matrix (7,396 bp) that includes PCG12 and the two rRNA genes, totaling 8,945 bp. All matrices underwent analysis using maximum likelihood (ML) with RAxML (version 8.2.12) [41] and Bayesian inference (BI) with MrBayes (version 3.2.7a) [42]. PartitionFinder2 (version 2.1.1) [43] was employed to identify the optimal partitioning schemes and substitution models. Both ML and BI analyses were performed on both partitioned and non-partitioned data to construct the phylogenetic trees. For the ML analysis, the "GTRGAMMA" nucleotide substitution model was selected, and a bootstrap analysis with 1000 replicates was conducted. In the BI analysis, four simultaneous Markov chain Monte Carlo (MCMC) runs of 100 million generations each were executed, with trees sampled every 2000 generations. The first 25% of the steps were discarded as burn-in. Stationarity was deemed achieved when the average standard deviation of split frequencies

 doi:10.20944/preprints202504.2155.v1

dropped below 0.01. The resulting trees from all analyses were visualized and edited using iTOL (https://itol.embl.de) [44].

3. Results

3.1. Genome Organization

The complete mitochondrial genomes of *Microtendipes* species have been successfully sequenced. These genomes consist of double-stranded circular molecules, with sizes ranging from 15,756 bp (PP966950) to 16,340 bp (PP966952). Each genome encodes a total of 37 genes, comprising 13 protein-coding genes (PCGs), 2 ribosomal RNA (rRNA) genes, and 22 transfer RNA (tRNA) genes, as detailed in Table 1. The primary source of length variation among these genomes is the control region, which exhibits a size range from 338 bp (PP966951) to 1,266 bp (PP966952). Regarding the coding sequences, minimal variation is observed in the lengths of the PCGs, tRNAs, and rRNAs. Specifically, the PCGs span from 11,106 bp (PP966952) to 11,154 bp (PP966949), the tRNAs range from 1,575 bp (PP966952) to 1,595 bp (PP966949), and the rRNAs vary between 1,488 bp (PP966950) and 1,508 bp (PP966949). Notably, these 37 genes maintain a consistent order across all nine genomes examined. Furthermore, 23 of these genes (including 9 PCGs and 14 tRNAs) are encoded by the majority strand (J-strand), while the remaining genes are encoded by the minority strand (N-strand), as illustrated in Figure 1.

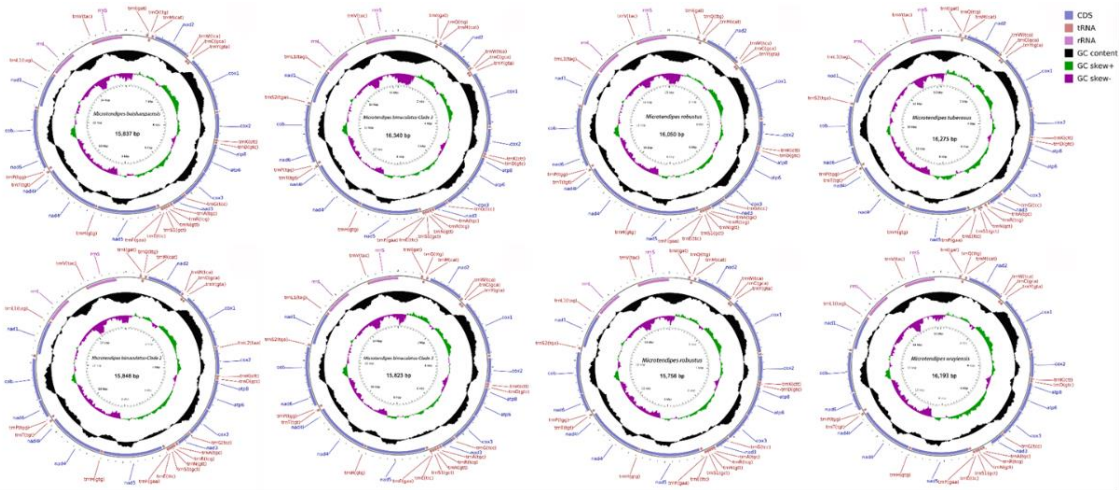

Figure 1. The mitogenome map depicted the distinctive mitochondrial genome attributes of various representative species of *Microtendipes*.

Table 2. Nucleotide composition of nine *Microtendipes* mitogenomes.

Species	Whole Genome					PCG					tRNA				
	Length (bp)	AT%	AT-Skew%	GC%	GC-Skew%	Length (bp)	AT%	AT-Skew%	GC%	GC-Skew%	Length (bp)	AT%	AT-Skew%	GC%	GC-Skew%
M. bimaculatus	15827	80.41	1.08	19.59	-18.13	11121	77.84	-17.69	22.16	1.62	1578	82.76	-3.67	17.24	29.41
M. bimaculatus	15848	80.1	1.88	19.9	-18.87	11121	77.63	-17.66	22.37	0.88	1583	82.56	-3.76	17.44	28.99
M. bimaculatus	16340	80.28	2.62	19.72	-20.73	11106	77.06	-17.91	22.94	-1.65	1575	82.67	-3.69	17.33	29.67
M. bimaculatus	15823	79.76	2.66	20.24	-20.3	11106	77.02	-17.94	22.98	-1.57	1583	82.82	-3.43	17.18	30.15
M. baishanzuensis	15837	80.35	2.08	19.65	-19.54	11121	77.8	-17.32	22.2	1.90	1577	82.18	-3.70	17.82	31.67
M. tuberosus	16257	79.97	2.61	20.03	-19.74	11154	76.94	-19.16	23.06	0.16	1595	82.88	-2.43	17.12	27.47

 doi:10.20944/preprints202504.2155.v1

M. robustus	15756	80.12	2.10	19.88	-18.97	11109	77.5	-18.04	22.5	0.56	1593	82.93	-2.95	17.07	29.41
M. robustus	16050	80.77	1.67	19.23	-18.04	11109	78.09	-17.92	21.91	2.38	1582	82.62	-3.29	17.38	31.64
M. wuyiensis	16193	79.19	2.34	20.81	-22.26	11118	76.07	-18.13	23.93	0.56	1587	82.61	-3.16	17.39	28.99

Species	rRNA					CR				
	Length (bp)	AT%	AT-Skew%	GC%	GC-Skew%	Length (bp)	AT%	AT-Skew%	GC%	GC-Skew%
M. bimaculatus	1492	82.44	5.05	17.56	12.98	726	94.9	-8.27	5.1	-56.76
M. bimaculatus	1494	82.26	4.48	17.74	16.23	408	94.36	-2.33	5.64	-47.83
M. bimaculatus	1496	82.29	4.79	17.71	13.96	1266	94.55	0.58	5.45	-62.32
M. bimaculatus	1498	82.31	4.94	17.69	13.96	922	94.14	0	5.86	-55.56
M. baishanzuensis	1492	82.51	4.30	17.49	13.41	798	94.74	-9.52	5.26	-57.14
M. tuberosus	1508	81.43	3.92	18.57	14.29	664	94.58	5.41	5.42	-72.22
M. robusts	1488	82.39	4.73	17.61	15.27	727	96.42	0.72	3.58	-53.85
M. robusts	1490	82.42	5.05	17.58	13.74	615	95.45	-0.85	4.55	-35.71
M. wuyiensis	1501	81.48	5.65	18.52	12.23	338	95.56	-3.41	4.44	-46.67

3.2. Nucleotide Composition

The nucleotide compositions of the nine mitochondrial genomes exhibit considerable similarity, as outlined in Table 2. The AT content varies between 79.19% in *Microtendipes wuyiensis* (PP966951) and 80.77% in *Microtendipes robustus* (PP966954). Notably, the AT content within the control region is significantly elevated compared to the entire genome, with a range from 94.14% in *Microtendipes bimaculatus* (PP966953) to 96.42% in *Microtendipes robustus* (PP966950). Similarly, the AT content in both rRNA and tRNA regions surpasses the overall genome level, with rRNA varying between 81.43% and 82.51%, and tRNA ranging from 82.18% to 82.93%. Conversely, the PCG sequences demonstrate a lower AT content, spanning from 76.07% in M*icrotendipes wuyiensis* to 78.09% in *Microtendipes robustus* (PP966954). All nine mitogenomes exhibit a positive AT-skew, ranging from 1.08% to 2.66%, and a negative GC-skew, varying between -22.26% and -18.04%. In contrast, the tRNA sequences display a negative AT-skew, ranging from -2.43% to -3.76%, and a positive GC-skew, spanning from 27.47% to 31.67%. The rRNA sequences exhibit positive AT-skew and GC-skew values, with ranges of 3.92% to 5.05% and 12.23% to 16.23%, respectively. For the PCG sequences, a notable negative AT-skew is observed, ranging from -17.31% to -19.16%, whereas the GC-skew is relatively insignificant, varying from -1.57% to 2.38%.

3.3. Protein-Coding Genes and Codon Usage

Among the 13 protein-coding genes (PCGs) in the nine mitochondrial genomes, 12 utilize ATG/ATT as their start codons. An exception is the cox1 gene, which employs ATA as the start codon in *Microtendipes wuyiensis* (PP966951) and TTG in the other eight mitogenomes. The nad1 gene in *Microtendipes wuyiensis* terminates with a TAG stop codon, whereas all other genes in the remaining mitochondrial genomes utilize TAA as their stop codon. Tables S1 and S2 provide the amino acid compositions and codon usage tables, respectively. Excluding stop codons, the total number of codons ranges from 3,689 to 3,705. Notably, the four *M. bimaculatus* mitogenomes contain 3,689, 3,689, 3,694, and 3,694 codons. The most frequently utilized codons are Leu (UUA), Phe (UUU), and Ile (AUU), as illustrated in Figure 2. It is worth mentioning that, with the exception of *Microtendipes bimaculatus* (Clade3), the AGG codon (encoding Ser) is absent in the other mitogenomes. Similarly, the CUG codon (encoding Leu) is absent in all mitogenomes except for *Microtendipes robustu* and *Microtendipes wuyiensis*. After excluding termination codons, the relative synonymous codon usage (RSCU) was calculated and summarized for the *Microtendipes* species, as shown in Figure 3.

 doi:10.20944/preprints202504.2155.v1

Additionally, we evaluated a suite of codon usage bias metrics, including the Codon Adaptation Index (CAI), Frequency of Optimal Codons (FOP), Effective Number of Codons (ENC), and GC content at the third codon position (GC3), which are detailed in Tables S3–S7. No significant differences were observed among the *Microtendipes* species in these metrics.

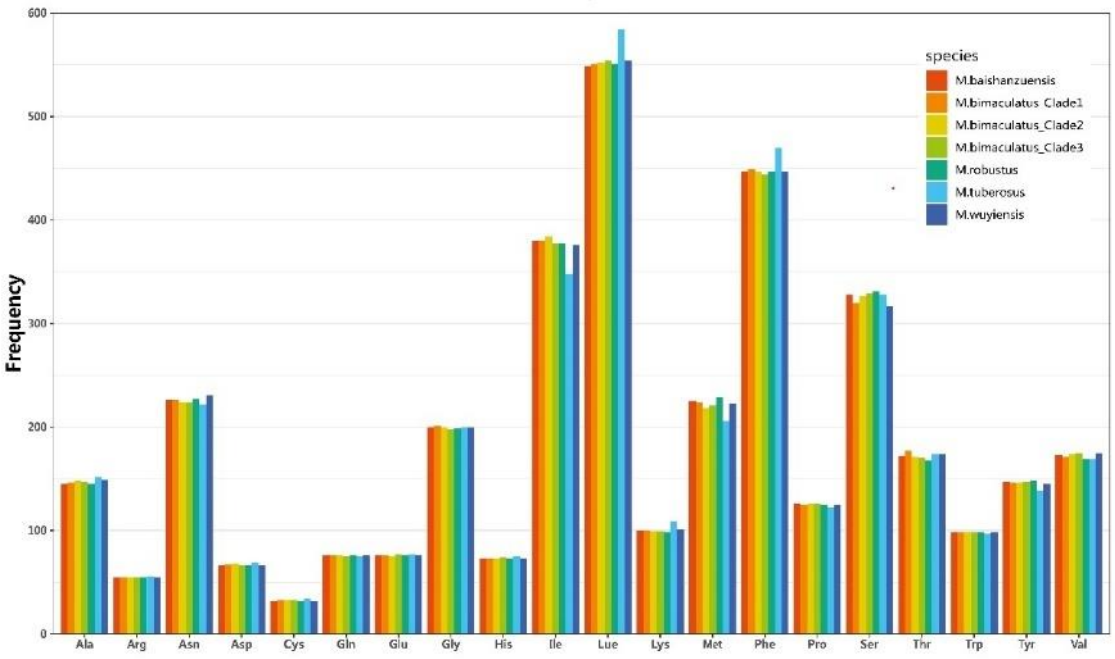

Figure 2. Amino acid frequency of PCGs in mitochondrial genomes of *Microtendipes* species.

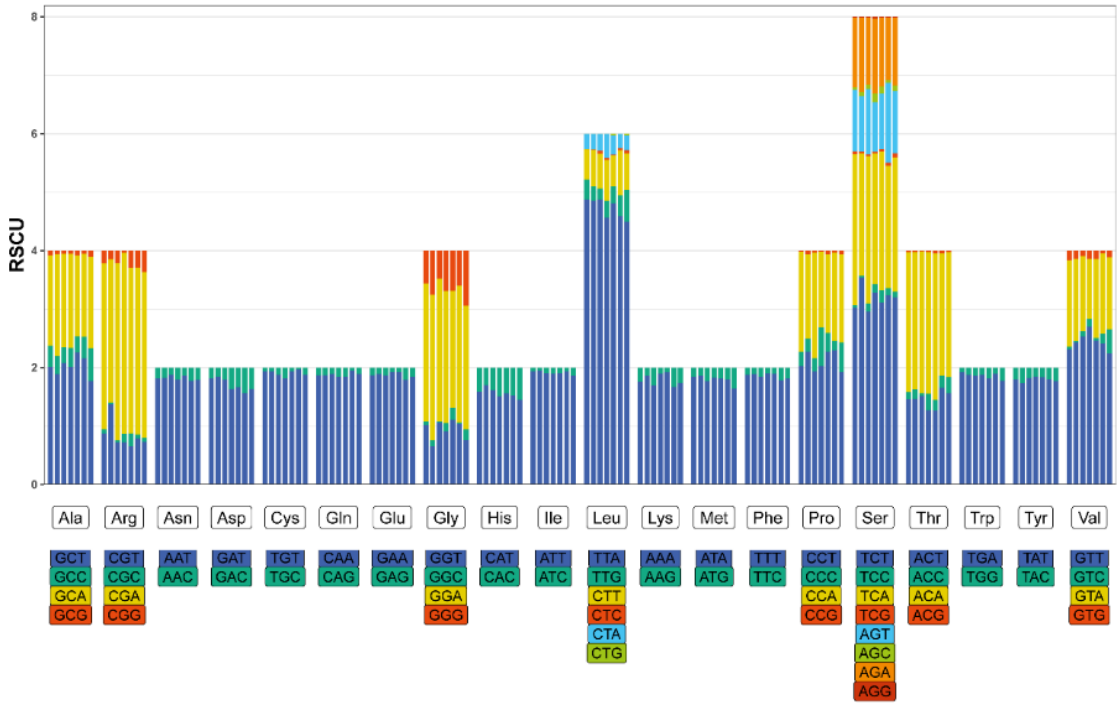

Figure 3. Relative synonymous codon usage (RSCU) of PCGs in mitochondrial genomes of Microtendipes species. The seven bars of each group represent *M. baishanzuensis*, *M. bimaculatus*_Clade1, *M. bimaculatus*_Clade2, *M. bimaculatus*_Clade3, *M. robustus*, *M. tuberosus*, and *M. wuyiensis*, separately.

 doi:10.20944/preprints202504.2155.v1

3.4. Phylogeny of Chironominae

In our analysis, all the generic complexes, such as the *Polypedilum* complex (excluding *Microtendipes*), *Chironomus* complex, and *Harnischia* complex, formed monophyletic groups (Figure 5 and Supplementary Trees S16-S23). The genus *Stenochironomus* exhibited instability in our phylogenetic trees, being either sister to other Chironominae species or to species within the *Polypedilum* complex. Similarly, the phylogenetic position of *Microtendipes* within Chironominae was unstable. Three primary topologies were constructed: (1) *Tanytarsus*, (*Polypedilum* complex, (*Microtendipes*, (*Harnischia* complex + *Chironomus* complex))), (2) *Tanytarsus*, ((*Chironomus* complex + *Harnischia* complex), (*Polypedilum* complex, *Microtendipes*)), and (3) *Tanytarsus*, (*Microtendipes*, (*Polypedilum* complex, (*Chironomus* complex + *Harnischia* complex))), with the last one resembling that proposed by Sæther (1977).

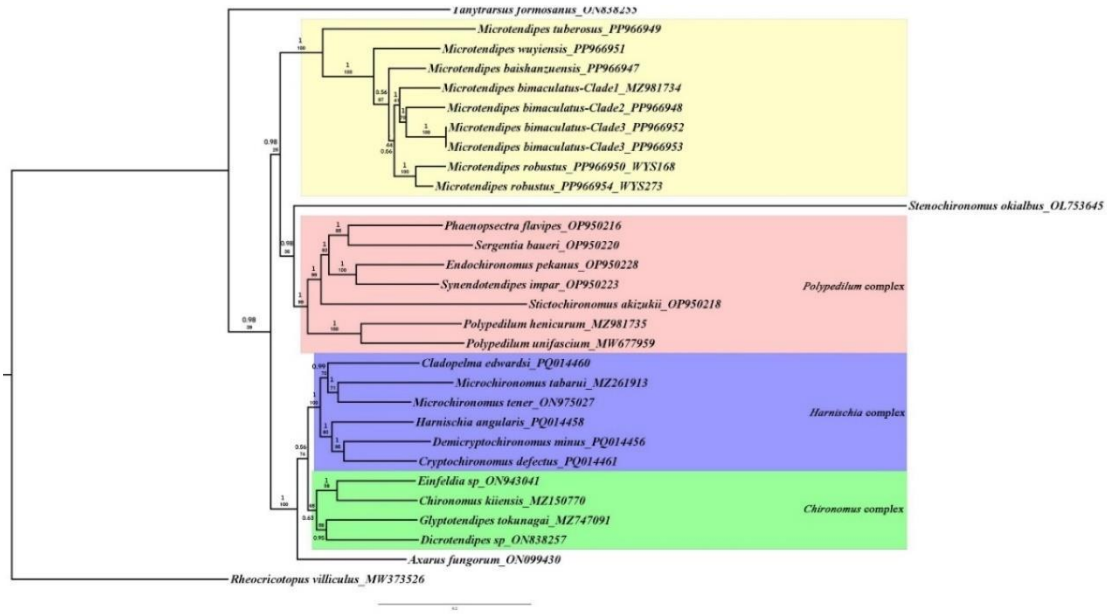

Figure 4. Phylogenetic tree of Chironominae species based on Mitogenome sequences. Values- up on branch present bootstrap supports (%) and Values-down are Bayesian posterior probabilities (PP).

4. Discussion

4.1. 658 bp COI Based Barcode vs Mitogenome-Based Barcode

The 658bp COI barcode has been instrumental in advancing our understanding of species diversity by leveraging its high level of sequence variation and ease of amplification. However, as our understanding of species complexity deepens, the limitations of this barcode have become increasingly apparent. One potential problem exposed by DNA barcodes is the excessive division of species especially in some super diverse genus, e.g. *Tanytarsus* and *Polypedilum* [30, 46]. Whereas in Song et al. (2023) *Microtendipes bimaculatus* Song et Qi, with deep intraspecific genetic divergence and forming three paraphyletic clades in phylogenic tree [24]. It is difficult to judge whether there are potential cryptic species in this species group based on the overall situation at that time. While in this study, four specimens mitogenomes from the three clades were used, for *Microtendipes bimaculatus*-clade 1 (MZ981734); *Microtendipes bimaculatus*-clade 2 (PP966948); *Microtendipes bimaculatus*-clade 3 (PP966952 and PP966953), with the genetic distance up to 10.6%. We try to compare the genetic difference between different protein coding genes. The genetic distances were reassessed individually based on 13 protein-coding genes (PCGs), as detailed in Supp. table S8 to S21. The intraspecific distances varied considerably, spanning from 5.3% for NAD4L, 7.0% for NAD1, 7.2% for NAD2, 8.8% for NAD4, 8.2% for NAD5, 9.0% for NAD3, 9.3% for COI, 9.5% for COII, 9.6% for ATP6,

 doi:10.20944/preprints202504.2155.v1

10.0% for COB, 10.0% for NAD6, 10.1% for COIII, to 13.8% for ATP8. Judging from distance-threshold methods, such as insect species proposes a threshold of 2–3%; however, genus-specific thresholds have been suggested for some Chironomidae including 4–5% for *Tanytarsus* [46] and 5–8% for *Polypedilum* [30]. Such single gene-based barcodes might mislead when closely related species deep intraspecific splits [46–47]. We also constructed phylogenetic trees to infer the relationships among *Microtendipes* species separately, using each coding gene, the concatenated 13-protein coding mitogenome genes, and all mitogenome sequences to infer their phylogeny (Supplementary Trees S1-S15). Only the trees based on nad3 and nad4 supported the monophyly of *Microtendipes bimaculatus*, albeit with low bootstrap values. Therefore, they should be considered part of the *Microtendipes bimaculatus* species complex, as defined by Song et al. (2023), or sibling species that are difficult to distinguish morphologically [24]. The other divergent species, *Microtendipes robustus* (PP966950 versus PP966954), formed robust relationships. Further analysis of the variance among different genes was conducted (Figure 4). The pairwise genetic distances of 13 PCGs across nine specimens were computed. For the majority of PCGs, the genetic distances remained statistically indistinguishable. However, two notable exceptions were observed: the genetic distance of ATP8 was significantly higher compared to that of all other PCGs, whereas the genetic distance of nad4l was markedly lower than that of its counterparts.

While the 658bp COI barcode has served as a valuable foundation for species identification and biodiversity research, the mitogenome-based barcode offers a promising alternative that may prove to be more suitable for certain applications. The mitogenome-based barcode's primary advantage lies in its ability to harness the vast genetic information contained within the mitochondrial genome. This allows for a more nuanced and accurate assessment of species relationships. Furthermore, the mitogenome-based barcode's comprehensive nature enables researchers to delve deeper into the evolutionary history and population dynamics of species, providing insights that can inform conservation efforts and management strategies.

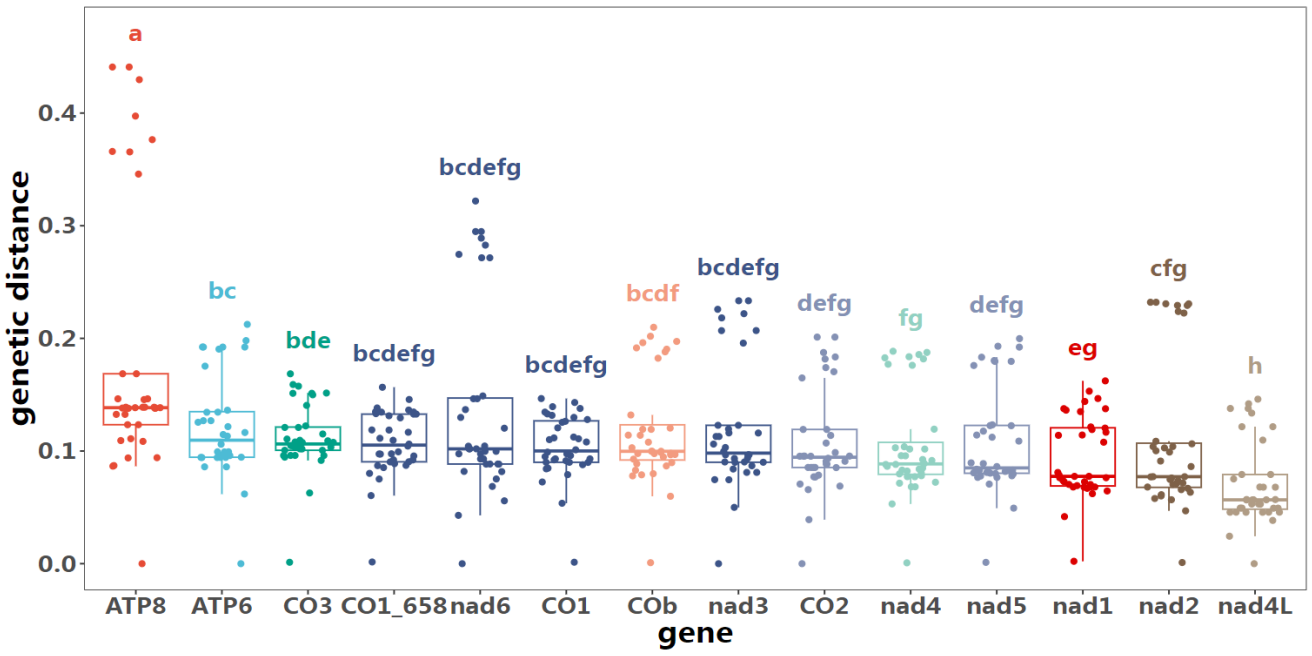

Figure 4. The genetic distance of PCGs between 9 specimens. CO1_658 represents the 658 bp COI barcode.

4.2. Phylogenetic Position of Microtendipes

In our analysis, all the generic complexes, such as the *Polypedilum* complex (excluding *Microtendipes*), *Chironomus* complex, and *Harnischia* complex, formed monophyletic groups (Figure 5 and Supplementary Trees S16-S23). The genus *Stenochironomus* exhibited instability in our

 doi:10.20944/preprints202504.2155.v1

phylogenetic trees, being either sister to other Chironominae species or to species within the *Polypedilum* complex. Similarly, the phylogenetic position of *Microtendipes* within Chironominae was unstable. Three primary topologies were constructed: (1) *Tanytarsus*, (*Polypedilum* complex, (*Microtendipes*, (*Harnischia* complex + *Chironomus* complex))), (2) *Tanytarsus*, ((*Chironomus* complex + *Harnischia* complex), (*Polypedilum* complex, *Microtendipes*)), and (3) *Tanytarsus*, (*Microtendipes*, (*Polypedilum* complex, (*Chironomus* complex + *Harnischia* complex))), with the last one resembling that proposed by Sæther (1977) [26]. This similarity suggests that *Microtendipes* and its related taxa may constitute a generic complex or potentially represent the fourth tribe within this subfamily. Dataset (iii) proposed a relationship of (*Chironomus* complex (*Polypedilum* complex (*Tanytarsus*, *Microtendipes*))), which does not align ideally with current taxonomy. Specifically, the positioning of Tanytarsus within the Chironomini tribe is incongruent, whereas the similar relationship between *Microtendipes* and *Tanytarsus* echoes observations made by Cranston et al. (2012) [28]. Importantly, most results do not support the inclusion of *Microtendipes* within the *Polypedilum* complex, thereby refuting the categorization proposed by Sasa (1989) [27]. Given the absence of mitochondrial genome data for Pseudochironomini, we are currently unable to conclusively determine the genus's taxonomic status. Nonetheless, we are committed to expanding our study by incorporating additional taxa from Tanytarsini and Pseudochironomini, aiming to unravel the precise phylogenetic positioning of *Microtendipes* with greater accuracy.

4.3. Phylogeny Within Microtendipes

The phylogenetic relationships within the genus *Microtendipes* have persisted as an enigmatic puzzle, particularly concerning the subdivision into species groups. Two distinct species groups, the *pedellus* group and the *rydalensis* group, were established based on larval stages, utilizing two pivotal characters: the number of premandibular teeth and the shape of a median tooth on the mentum [48]. According to this diagnostic criterion, *M. baishanzuensis* is classified within the *rydalensis* group, whereas *Microtendipes tuberosus* and *Microtendipes robustus* are assigned to the *pedellus* group (unpublished data). However, it is evident that this classification system does not align seamlessly with the phylogenetic tree, as *Microtendipes tuberosus* occupies a basal position within the genus's clade, while other species occupy distinct and separate clades (Figure 5). This discrepancy underscores the need for further investigation to clarify the evolutionary relationships and taxonomic structure within the genus *Microtendipes*.

5. Conclusions

All eight newly sequenced mitogenomes in this study demonstrated a striking congruity in their structural features and nucleotide compositions when juxtaposed against previously published Chironomidae data. The mitogenome-based species delimitation within the genus *Microtendipes* offers a more precise and nuanced perspective than COI-based barcoding, particularly those that involve substantial intraspecific genetic distances. The comparative analysis of *Microtendipes* (Diptera: Chironomidae) mitogenomes has yielded invaluable insights into their phylogenetic relationships, which do not support two species group division based on larvae. This analysis also has definitively refuted the placement of *Microtendipes* within the *Polypedilum* complex, instead tentatively establishing it as a distinct species group and tribe, thereby advancing our understanding of this intriguing taxonomic entity.

Supplementary Materials: The following supporting information can be downloaded at the website of this paper posted on Preprints.org, Table S1 Amino acids composition of Microtendipes; Table S2 codon usage of Microtendipes; Table S3 codon adaptation index of Microtendipes; Table S4 frequency of optical codons of Microtendipes; Table S5 effective number of codon of Microtendipes; Table S6 base composition by position of Microtendipes; Table S7 relative synonymous codon usage of Microtendipes; Table S8 Genetic divergences based on ATP6; Table S9 Genetic divergences based on ATP8; Table S10 Genetic divergences based on Cob; Table S11 Genetic divergences based on CO1; Table S12 Genetic divergences based on CO1-658; Table S13 Genetic divergences based on COII; Table S14 Genetic divergences based on CO3; Table S15 Genetic divergences based

 doi:10.20944/preprints202504.2155.v1

on nad1; Table S16 Genetic divergences based on nad2; Table S17 Genetic divergences based on nad3; Table S18 Genetic divergences based on nad4; Table S19 Genetic divergences based on na4L; Table S20 Genetic divergences based on nad5; Table 21 Genetic divergences based on nad6; Tree S1 ML tree based on ATP6; Tree S2 ML tree based on ATP8; Tree S3 ML tree based on COi; Tree S4 ML tree based on COii; Tree S5 ML tree based on CO3; Tree S6 ML tree based on COb; Tree S7 ML tree based on nad1; Tree S8 ML tree based on nad2; Tree S9 ML tree based on nad3; Tree S10 ML tree based on nad4; Tree S11 ML tree based on nad4L; Tree S12 ML tree based on nad5; Tree S13 ML tree based on nad6; Tree S14 BI tree based on protein coding genes; Tree S15 BI tree based on mitogenome genes; Tree S16 ML tree based protein coding genes without partition; Tree S17 ML tree based protein coding genes codon 1st and Condon 2nd without partition; Tree S18 ML tree-based protein coding genes codon 1st and Condon 2nd and rDNA without partition; Tree S19 ML tree based protein coding genes and rDNA without partition; Tree S20 ML tree based protein coding genes with partition; Tree S21 ML tree based protein coding genes codon 1st and Condon 2nd with partition; Tree S22 ML tree based protein coding genes codon 1st and Condon 2nd and rDNA with partition; Tree S23 ML tree based protein coding genes and rDNA with partition.

Author Contributions: Performed the experimental procedures and data collection: Wenji Wang, Yiyi Wang, Teng Lei, and Chao Song. Conceived and designed the research project: Luxian Li and Xin Qi. Analyzed the data and wrote the manuscript: Chao Song, Luxian Li, and Xin Qi. All authors have read and approved the final manuscript for publication.

Funding: This research was funded by the National Natural Science Foundation of China (NSFC, Grant No. 32100353, 32070481) and the Zhejiang Provincial Natural Science Foundation of China (Grant No. LY22C040003).

Institutional Review Board Statement: Not applicable.

Data Availability Statement: Data supporting this study are available in the article and accompanying online supplementary material, and in NCBI GenBank (https://www.ncbi.nlm.nih.gov/) under the following accession numbers (PP966947-PP966954).

Conflicts of Interest: The authors declare no conflicts of interest.

References

1. Cameron, S.L. Insect Mitochondrial Genomics: Implications for Evolution and Phylogeny. *Annu. Rev. Entomol.* **2014,** *59*, 95–117.
2. Chen, L.P.; Zheng, F.Y.; Bai, J.; Wang, J.M.; Li, X.J. Comparative analysis of mitogenomes among six species of grasshoppers (Orthoptera: Acridoidea: Catantopidae) and their phylogenetic implications in wing-type evolution. *Int. J. Biol. Macromol.* **2020,** *159*, 1062–1072.
3. Jiang, J.; Chen, X.; Li, C.; Song, Y.H. Mitogenome and phylogenetic analysis of typhlocybine leafhoppers (Hemiptera: Cicadellidae). *Sci. Rep*. **2021**, *11(1)*, 10053.
4. Zheng, C.; Zhu, X.; Wang, Y.; Dong, X.; Yang, R.; Tang, Z.; Bu, W. Mitogenomes Provide Insights into the Species Boundaries and Phylogenetic Relationships among Three Dolycoris Sloe Bugs (Hemiptera: Pentatomidae) from China. *Insects*. **2024**, *15*, 134.
5. Mohamed, W.M.A.; Moustafa, M.A.M.; Thu, M.J.; et al. Comparative mitogenomics elucidates the population genetic structure of Amblyomma testudinarium in Japan and a closely related Amblyomma species in Myanmar. *Evol. appl.* **2022,** *15(7),* 1062-1078.
6. Yamamoto, K.; Sakaue, S.; Matsuda, K.; et al. Genetic and phenotypic landscape of the mitochondrial genome in the Japanese population. *Commun. Biol.* **2020,** *3*, 104.
7. Boore, J.L. Animal mitochondrial genomes. *Nucleic. Acids. Res.* **1999**, *27*, 1767–1780.
8. Finstermeier, K.; Zinner, D.; Brameier, M.; et al. A mitogenomic phylogeny of living primates. *PloS. one.* **2013**, *8(7)*, e69504.
9. Ma, Q.; Li, F.; Zheng, J.; Liu, C.; Wang, A.; Yang, Y.; Gu, Z. Mitogenomic phylogeny of Cypraeidae (Gastropoda: Mesogastropoda). *Front Ecol Evol.* **2023**, *11*, 1138297.
10. Irwin, A.R.; Strong, E.E.; Kano, Y.; Harper, E.M.; Williams, S.T. Eight new mitogenomes clarify the phylogenetic relationships of Stromboidea within the caenogastropod phylogenetic framework. *Mol. Phylogenet. Evol.* **2021**, *158*, 107081.
11. Phillips, M.J.; Zakaria, S.S. Enhancing mitogenomic phylogeny and resolving the relationships of extinct megafaunal placental mammals. *Mol. Phylogenet. Evol.* **2021**, *158*, 107082.

 doi:10.20944/preprints202504.2155.v1

12. Poliseno, A.; Feregrino, C.; Sartoretto, S.; Aurelle, D.; Wörheide, G.; McFadden, CS.; Vargas, S. Comparative mitogenomics, phylogeny and evolutionary history of Leptogorgia (Gorgoniidae). *Mol. Phylogenet. Evol.* **2017**, *115*,181–189.
13. Timmermans, M.J.T.N.; Lees, D.C.; Simonsen, T.J. Towards a mitogenomic phylogeny of Lepidoptera. *Mol. Phylogenet. Evol.* **2014**, *79*,169–178.
14. Fang, X.; Wang, X.; Mao, B.; et al. Comparative mitogenome analyses of twelve non-biting flies and provide insights into the phylogeny of Chironomidae (Diptera: Culicomorpha). *Sci. Rep.* **2023**, *13(1)*, 9200.
15. Li, S.Y.; Chen, M.H.; Sun, L.; Wang, R.H.; Li, C.H.; Gresens, S.; Li, Z.; Lin, X.L. New mitogenomes from the genus Cricotopus (Diptera: Chironomidae, Orthocladiinae): Characterization and phylogenetic implications. *Arch Insect Biochem Physiol*. **2024**, *115(1)*, e22067.
16. Lin, X.L.; Liu, Z.; Yan, L.P.; Duan, X.; Bu, W.J.; Wang, X.H.; Zheng, C.G. Mitogenomes provide new insights of evolutionary history of Boreheptagyiini and Diamesini (Diptera: Chironomidae: Diamesinae). *Ecol Evol.* **2022**, *12(5)*, e8957.
17. Zhang, D.; He, F.X.; Li, X.B.; Aishan, Z.; Lin, X.L. New mitogenomes of the Polypedilum generic complex (Diptera: Chironomidae): characterization and phylogenetic implications. *Insects.* **2023**, *14(3)*, 238.
18. Kawai, K.; Kawaguchi, K.; Kodama, A.; Saito, H. Fundamental studies on acid-tolerant chironomids in Japan. *Limnology*. **2019**, *20*, 101–107.
19. Pinder, L.C.V. Biology of freshwater Chironomidae. *Annu Rev Entomol*. **1986**, *31(1)*, 1-23.
20. Martel-Cea, A.; Astorga, G.A.; Hernández, M.; Caputo, L.; Abarzúa, A.M. Modern chironomids (Diptera: Chironomidae) and the environmental variables that influence their distribution in the Araucanian lakes, south-central Chile. *Hydrobiologia.* **2021**, *848*, 2551–2568.
21. Kozeretska, I.; Serga, S.; Kovalenko, P.; Gorobchyshyn, V.; Convey, P. Belgica antarctica (Diptera: Chironomidae): A natural model organism for extreme environments. *Insect Science.* **2022**, *29(1*), 2–20.
22. Qi, X.; Wang, X.H. A review of Microtendipes Kieffer from China (Diptera: Chironomidae). *Zootaxa.* **2006**, *1108(1)*, 37–51.
23. Tang, H.; Niitsuma, H. Review of the Japanese Microtendipes (Diptera: Chironomidae: Chironominae), with description of a new species. *Zootaxa.* **2017**, *4320(3*), 535–553.
24. Song, C.; Wang, L.; Lei, T.; Qi, X. New color-patterned species of Microtendipes Kieffer, 1913 (Diptera: Chironomidae) and a deep intraspecific divergence of species by DNA barcodes. *Insects.* **2023**; *14(3),* 227.
25. Cao, J.K.; Lei, T.; Gu, J.J.; Song, C.; Qi, X. Codon bias analysis of the mitochondrial genome reveals natural selection in the nonbiting midge Microtendipes umbrosus Freeman, 1955 (Diptera: Chironomidae). *The Pan-Pacific Entomologist*. **2023**, *99(4)*, 217–225.
26. Sæther, O.A. Female genitalia in Chironomidae and other Nematocera: morphology, phylogenies, keys. *Bull Fish Res Board Can.* **1977**, *197,* 1–209.
27. Sasa, M. Chironomidae of Japan: Checklist of species recorded, key to males and taxonomic notes. *NIES Res Rep*. **1989**, *125*,1–177.
28. Cranston, P.S.; Hardy, N.B.; Morse, G.E. A dated molecular phylogeny for the Chironomidae (Diptera). *Syst Entomol*. **2012**, *37(1)*, 172–188.
29. Folmer, O.; Black, M.; Hoeh, W.; Lutz, R.; Vrijenhoek, R. DNA primers for amplification of mitochondrial oxidase subunit I from diverse metazoan invertebrates. *Mol Mar Biol Biotechnol*. **1994**, *3(5)*,294–299.
30. Song, C.; Lin, X.L.; Wang, Q.; Wang, XH. DNA barcodes successfully delimit morphospecies in a superdiverse insect genus. *Zool Scr*. **2018**, *47(3)*, 311–324.
31. Meng, G.; Li, Y.; Yang, C.; Liu, S. MitoZ: a toolkit for animal mitochondrial genome assembly, annotation and visualization. *Nucleic Acids Res.* **2019**, *47(11)*, e63.
32. Dierckxsens, N.; Mardulyn, P.; Smits, G. NOVOPlasty: De novo assembly of organelle genomes from whole genome data. *Nucleic Acids Res.* **2017**, *45(4)*, e18.
33. Prjibelski, A.; Antipov, D.; Meleshko, D.; Lapidus, A.; Korobeynikov, A. Using SPAdes de novo assembler. *Current Protocols in Bioinformatics.* **2020**, *70(1)*, e102.
34. Stothard, P.; Wishart, D.S.; Circular genome visualization and exploration using CGView. *Bioinformatics*. **2005**, *21*,537-539.

 doi:10.20944/preprints202504.2155.v1

35. Donath, A.; Jühling, F.; Al-Arab, M.; Bernhart, S.H.; Reinhardt, F.; Stadler, P.F.; Middendorf, M.; Bernt, M. Improved annotation of protein-coding genes boundaries in metazoan mitochondrial genomes. *Nucleic Acids Res.* **2019**, *47*, 10543–10552.
36. Shen, W.; Sipos, B.; Zhao, L. SeqKit2: A Swiss army knife for sequence and alignment processing. *iMeta*. **2024**, *5*, e191.
37. Rice, P.; Longden, I.; Bleasby, A. EMBOSS: the European molecular biology open software suite. *Trends in genetics.* **2000**, *16(6)*, 276-277.
38. Wickham, H.; Chang, W.; Wickham, M.H. Package 'ggplot2'. Create elegant data visualisations using the grammar of graphics. *Version*. **2016**, *2(1)*, 1–189.
39. Katoh, K.; Standley, D.M. MAFFT multiple sequence alignment software version 7: improvements in performance and usability. *Molecular biology and evolution*. **2013**, *30(4)*, 772–780.
40. Tamura, K.; Stecher, G.; Kumar, S. MEGA11: Molecular evolutionary genetics analysis version 11. *Mol Biol Evol.* **2021**, *38*, 3022–3027.
41. Stamatakis, A. RAxML version 8: a tool for phylogenetic analysis and post-analysis of large phylogenies. *Bioinformatics.* **2014**, *30(9)*, 1312–1313.
42. Ronquist, F.; Teslenko, M.; Van der Mark, P.; Ayres, D.L.; Darling, A.; Höhna, S.; Larget, B.; Liu, L.; Suchard, M.A.; Huelsenbeck, J.P. MRBAYES 3.2: Efficient Bayesian phylogenetic inference and model selection across a large model space. *Syst. Biol.* **2012**, *61(3)*, 539–542.
43. Lanfear, R.; Frandsen, P.B.; Wright, A.M.; Senfeld, T.; Calcott, B. PartitionFinder 2: new methods for selecting partitioned models of evolution for molecular and morphological phylogenetic analyses. *Mol Biol Evol.* **2017**, *34(3)*, 772–773.
44. Letunic, I.; Bork, P. Interactive Tree of Life (iTOL) v5: an online tool for phylogenetic tree display and annotation. *Nucleic Acids Res.* **2021**, *49(W1)*, W293–296.
45. Lin, X.L.; Stur, E.; Ekrem, T. Exploring genetic divergence in a species-rich insect genus using 2790 DNA barcodes. *PLoS. One*. **2015**, *10(9)*, e0138993.
46. Meier, R.; Shiyang, K.; Vaidya, G.; Ng, PKL. DNA barcoding and taxonomy in diptera: A tale of high intraspecific variability and low identification success. *Syst Biol*. **2006**, *55(5)*, 715–728.
47. Yeo, D.; Puniamoorthy, J.; Ngiam, R.W.; Meier, R. Towards holomorphology in entomology: rapid and cost-effective adult–larva matching using NGS barcodes. *Syst. entomol.* **2018**, *43(4)*, 678–691.
48. Epler, J.H.; Ekrem, T.; Cranston, P.S. "10. The larvae of Holarctic Chironominae (Diptera: Chironomidae)–Keys and diagnoses." *Chironomidae of the Holarctic Region. Keys and diagnoses. Part 1.* **2013**, 387–556.